Redox driven conductance changes for resistive memory

Lian C.T. Shoute · Nikola Pekas · Yiliang Wu ·
Richard L. McCreery

Abstract The relationship between bias-induced redox reactions and resistance switching is considered for memory devices containing TiO_2 or a conducting polymer in "molecular heterojunctions" consisting of thin (2–25 nm) films of covalently bonded molecules, polymers, and oxides. Raman spectroscopy was used to monitor changes in the oxidation state of polythiophene in Au/P3HT/SiO_2/Au devices, and it was possible to directly determine the formation and stability of the conducting polaron state of P3HT by applied bias pulses [P3HT = poly(3-hexyl thiophene)]. Polaron formation was strongly dependent on junction composition, particularly on the interfaces between the polymer, oxide, and electrodes. In all cases, trace water was required for polaron formation, leading to the proposal that water reduction acts as a redox counter-reaction to polymer oxidation. Polaron stability was longest for the case of a direct contact between Au and SiO_2, implying that catalytic water reduction at the Au surface generated hydroxide ions which stabilized the cationic polaron. The spectroscopic information about the dependence of polaron stability on device composition will be useful for designing and monitoring resistive switching memory based on conducting polymers, with or without TiO_2 present.

L.C.T. Shoute · N. Pekas · R.L. McCreery (✉)
National Institute for Nanotechnology, 11421 Saskatchewan Dr.,
Edmonton, Alberta, Canada, T6G 2M9
e-mail: mccreery@ualberta.ca

L.C.T. Shoute · R.L. McCreery
Department of Chemistry, University of Alberta, 11227
Saskatchewan Dr., Edmonton, Alberta T6G 2G2, Canada

Y. Wu
Xerox Research Centre of Canada, 2660 Speakman Drive,
Mississauga, Ontario, L5K 2L1, Canada

1 Introduction

As is well known to most readers of this special issue on resistive memories, a daunting array of examples of bias-induced conductance changes has been reported, with widely varying degrees of reproducibility and characteristics. Excellent reviews on organic resistive memories by Scott and Bozano [1], and inorganic conductance switching [2] have outlined both the range of materials and phenomena, as well as the difficulty of determining the mechanisms involved in resistive memory devices. Prominent in both reviews are "redox" reactions, in which an element of a memory device gains or loses electrons to cause a significant change in conductivity. Redox events are generally accompanied by ion motion to preserve electroneutrality, and may occur rapidly, in the submicrosecond range. Despite the many examples and hundreds of papers on resistive switching, the detailed mechanisms are often not clear, and the devices themselves have not matured commercially. Our group has considered redox reactions as the basis of conductance switching in "molecular heterojunctions" containing TiO_2 [3–6] or a conducting polymer [7], or both. We have proposed that "dynamic" doping induced by an applied bias can result in persistent changes in device conductance, and that the process may be useful for nonvolatile memory. Additional examples from the organic thin film transistor [8, 9] and conducting polymer [10–14] literature confirm the importance of redox reactions to resistive memory. Described herein are experiments intended to address a simple but important question: can redox reactions in "molecular heterojunctions" containing an organic thin film and a metal oxide underlie bias-induced conductance changes? We describe optical spectroscopy of a series of polymer/oxide heterojunctions to unequivocally establish redox events, and to investigate the device parameters and materials necessary for the occurrence of such phenomena.

Prominent examples of materials in which changes in oxidation state associated with reduction or oxidation (herein referred to as "redox") reactions can cause large changes in conductance include inorganic oxides such as TiO_2 and NiO and a large number of conducting polymers. A familiar example is polyacetylene, which is a poor conductor in its native state, but removal of an electron to form "polarons" increases the conductivity by 8–10 orders of magnitude [15–17]. Molecular iodine, I_2, is often used as the acceptor of the electron, with the conductive state being a polyacetylene polaron with its cationic charge compensated by an iodide anion. The process of polyacetylene oxidation by I_2 is generally referred to as "doping the polyacetylene with iodine", by analogy to inorganic semiconductors. Although the insertion of I^- into the polymer accompanies polaron formation, it is the oxidation itself which causes rehybridization of the polyacetylene to its conducting state. It is important to note that the identity of the anion has a minor effect on the conductivity change, as long as the polyacetylene backbone loses an electron to form the conducting polaron. Although the distinction is partly semantic, the oxidation of a polymer to its conducting state is quite a different phenomenon compared to adding an electron deficient element to a crystal to create a p-doped semiconductor, e.g. substitution doping of silicon with boron.

An inorganic example of a redox-induced conductance change which is relevant to the current paper is that of TiO_2. As is well known, TiO_2 is a semiconductor with a bulk conductivity of $<10^{-10}$ S/cm [18–20]. Reduction of TiO_2 to form Ti_2O_3 or TiO results in a large increase in conductivity to values approximately equal to that of Ti metal, i.e. >100 S/cm [3, 21]. The "extra" electrons from the reducing agent end up in the conduction band of the TiO_2 (the d-band), and they are therefore mobile. If electroneutrality is maintained during reduction, the TiO_2 must lose oxygen to become "oxygen deficient", or "n-doped", and is often represented as TiO_{2-x}, where x denotes the oxygen deficiency. Recent reports on the TiO_2 based "memristor" discuss mechanisms based on formation of a titanium "suboxide" such as Ti_4O_7, which is oxygen deficient and conductive [22–26]. Although the addition of electrons and the removal of oxygen (as O^{-2}) are coupled by the electroneutrality requirement, the conductivity and mobile electrons are the result of injection of electrons into the d-band in the TiO_2 lattice, and a decrease in the formal Ti oxidation state. We have reported a resistive memory device based on a heterojunction consisting of a thin layer of an organic molecule (fluorene, 2 nm thick) and a 10 nm layer of TiO_2 [3, 4, 6], as shown in Fig. 1a. A voltage scan of the device (Fig. 1b) revealed an increase in conductance when the Au was biased negative, with a "figure 8 hysteresis" characteristic of memory devices. Application of a 3 V, 50 msec bias pulse with the Au electrode negative results in transient reduction of

TiO_2 with a concomitant increase in conductance that persisted for $\sim$30 minutes (Fig. 1c). The conductance change in the device could be mimicked on a slower time scale by H_2 reduction causing a conductance increase, and the subsequent exposure to O_2 returning the device to the low conductance state (Fig. 1d). The observed conductance changes depended on the presence of H_2O, and they were absent in a vacuum or dry atmosphere. We concluded that the fluorene layer induced asymmetry into the device, permitting the applied bias to change the Fermi level within the TiO_2, and bring about the reduction of TiO_2 to the conducting "suboxide", TiO_{2-x} [3, 4]. Since the process was dependent on traces of H_2O, we proposed an electrochemical reaction induced by the bias pulse:

$$2TiO_2 + H_2O + 2e^- \rightarrow Ti_2O_3 + 2OH^- \qquad (1)$$
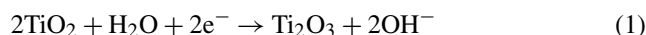
The Ti_2O_3 designation should be considered "formal", representing composition rather than structure, and may also be considered to be an oxygen vacancy. We note that the electron-beam deposited TiO_2 used in our devices is quite disordered, and should have a wider range of possible Ti oxidation states than crystalline rutile, anatase, or brookite.

Although the fluorene/TiO_2 device has several qualitative properties such as persistence, reversibility, and conductive readout which are attractive for nonvolatile memory applications, the switching speed and cycle life were inadequate for commercial applications. We have reported bias-induced redox reactions in the molecular layer of heterojunctions containing nitroazobenzene (NAB) [5, 27–29], and confirmed these changes with UV-Vis absorption and Raman spectroscopy [6, 30]. The spectroscopic changes correlated directly with changes in device conductance induced by an applied bias. A natural extension of the fluorene/TiO_2 device of Fig. 1a is a heterojunction containing two components capable of redox activity, both of which affect the device conductance. We reported a polypyrrole/TiO_2 device with promising memory performance in 2008 [7], and proposed that both the TiO_2 and the polypyrrole underwent significant changes in conductance in response to bias pulses. However, we have not reported in situ spectroscopic study of this device to correlate the redox properties of the polypyrrole and the device performance. The current paper describes investigation of the switching mechanism in related conducting polymer/oxide devices. We report herein spectroscopic investigations of such heterojunctions to test the postulate that redox reactions of the polymer can produce a metastable polaron state with potential value in nonvolatile memory applications. The main objective is determination of the switching mechanism and its dependence on the composition and properties of the component species, including the electrode materials.

Fig. 1 Resistance switching in carbon/fluorene/TiO_2/Au molecular heterojunctions. Panel **b** is a linear sweep (1 V/sec) current/voltage curve initiated in the positive direction from 0 volts. PPF is a pyrolyzed photoresist substrate. Panel **c**: negative voltage scans (1000 V/s) before and after bias pulses first to +3 than to −3 V. Panel **d**: JV curves (1000 V/s) obtained after exposure to H_2 and O_2 for several hours each. Figure adapted from reference [3]
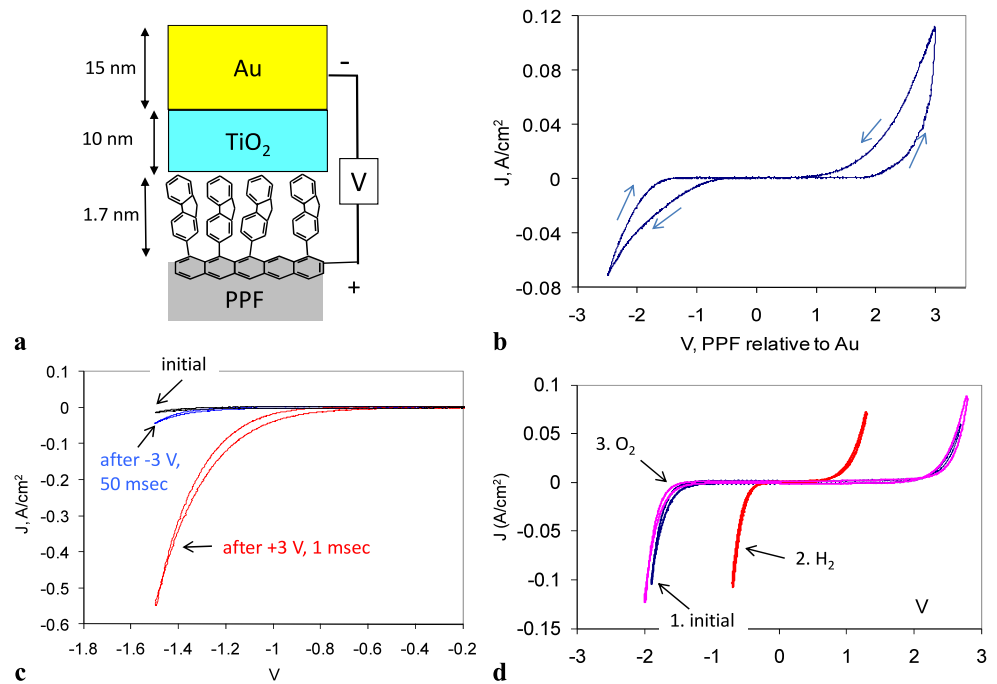
2 Experimental

Metals and oxides were deposited on a 300 nm thick layer of thermal SiO_2 on Si at $\sim 1 \times 10^{-6}$ Torr by electron-beam deposition, with mass thickness measured by a quartz microbalance adjacent to the sample. Junctions are designated by their sequence of layers from bottom to top, with the layer thickness in nm. For example, $Au/SiO_2(51)/P3HT(25)/Cr(2)/Au(10)$ designates a substrate of Au on Si/SiO_2, a 51 nm thick layer of e-beam deposited SiO_2, a 25 nm thick layer of P3HT, 2 nm of Cr, and 10 nm of Au. Bias values are always stated as the bottom electrode relative to top electrode, i.e. the bottom electrode is positive for positive bias pulses. Electronic grade regioregular poly(3-hexyl thiophene) (P3HT, MW $\sim$50,000) was obtained from Rieke metals, and spin coated onto the samples from a 0.5 w% P3HT solution in ortho-dichlorobenzene at 1000 RPM. The polymer thickness was determined to be $\sim$25 nm using AFM [31] for P3HT spun onto Au/SiO_2, and the P3HT thickness was assumed to be equal for the carbon and Au substrates. The device geometry was a "crossbar" with active regions 0.5×0.5 mm (area = 0.0025 cm²), and the edges of the polymer and oxide layers were exposed to the ambient atmosphere, including air, dry N_2, acetonitrile vapor, etc., as described in "Results" below. Raman spectra were obtained with a Thermo/Nicolet Raman microscope operating at 780 nm, with typically 2–10 second integration time on the CCD detector. Multivariate Curve Resolution (MCR) was performed in Matlab using PLS software from Eigenvector Research. The spectra were preprocessed by subtracting a linear baseline; then the MCR analysis was carried out with the only constraints being non-negative spectra and non-negative contributions. The analysis assumed two components contributed to each spectrum, but including a third component produced a third spectrum which was nearly identical to that of the second component. Using the data of Fig. 2 as an example, 96.4% of the variance was accounted for by two components, which increased to 98.5% for three components.

3 Results

We will consider first devices containing polythiophene as the conducting polymer, but no TiO_2. Polythiophene has a well defined Raman spectrum when excited with 780 nm light, as shown in Fig. 2a for poly(3-hexyl thiophene), designated as P3HT. The native, neutral form has a strong band at 1444 cm⁻¹, which shifts to 1405 cm⁻¹ when the polymer is oxidized to its polaron form. Although the oxidized, conducting state of P3HT can contain both a polaron and bipolaron, we will not distinguish between the two in this discussion. These peak frequencies vary somewhat with the solvent for solutions and processing methods for the solid [32–35]. The conductivities of the neutral and polaron form are $<10^{-7}$ S/cm and >1 S/cm, respectively [36, 37], depending on processing and atmosphere, and P3HT has been studied extensively due to its utility in organic photovoltaic devices [38–40]. The shift in the 1444 cm⁻¹ band upon oxidation and associated changes in smaller spectral features are good markers for polaron formation. Figure 2b shows Raman spectra of a $Au/SiO_2(50)/P3HT(25)/Cr(2)/Au(10)$ device obtained through the top Au electrode before and after
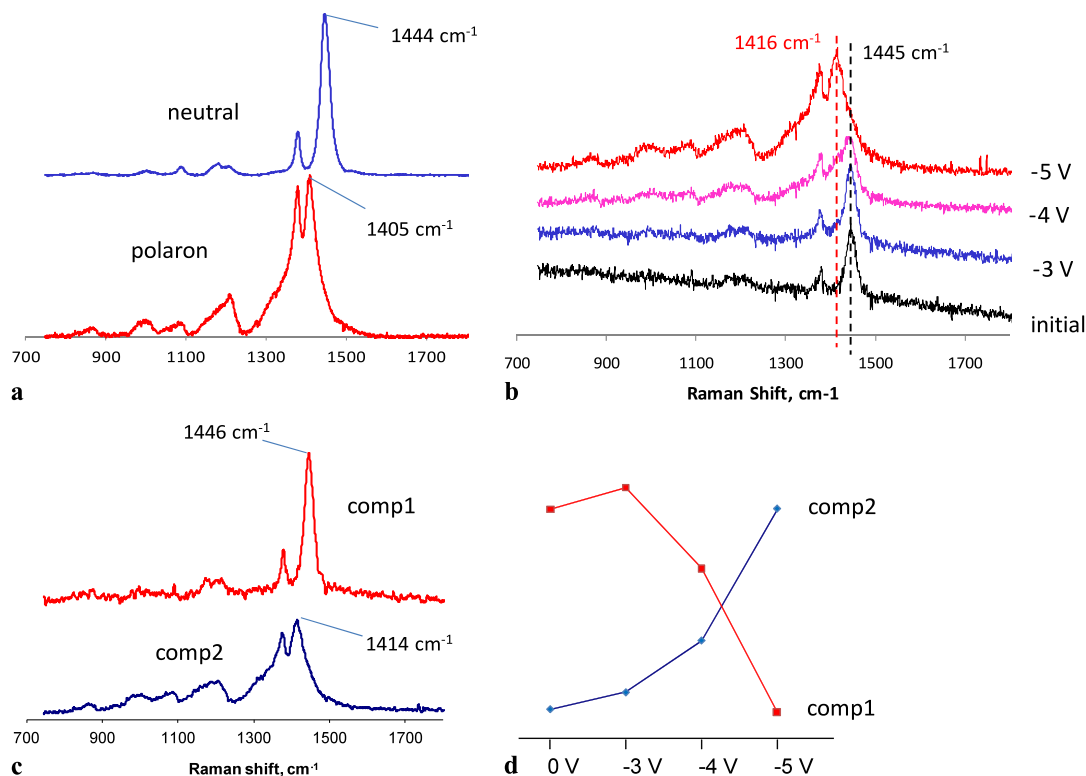
Fig. 2 a Raman spectra (780 nm laser) of solid, neutral P3HT (upper) and P3HT in chloroform following oxidation with FeCl$_3$. **b** Raman spectra obtained through the 10 nm Au contact of a Au/SiO$_2$(50)/P3HT(25)/Cr(2)/Au(10) device before and after 60 sec-ond bias pulses to the indicated voltages. **c** Components of a multivariate curve resolution (MCR) analysis of the spectra of panel **b**. **d** Relative contributions of the two MCR components for each spectrum

the device was biased for ∼60 sec at the indicated voltages, with the device at open circuit between bias pulses. The low conductivity of SiO$_2$ compared to TiO$_2$ serves to enhance redox effects in the polymer and to avoid redox processes attributable to TiO$_2$. Note that the thin layer of Cr significantly improves quality and reproducibility of the spectra by eliminating enhanced Raman effects at the Au surface. The progressively negative Au bottom electrode causes a visible change in the Raman spectrum, with a shift of the major peak from ∼1447 to ∼1405 cm^{-1}, indicating formation of the P3HT polaron. While these spectral changes are visible in the raw spectra, a more rigorous analysis uses multivariate curve resolution (MCR), as shown in Figs. 2c and 2d. The technique extracts the native spectra of the two components, and also provides quantitative assessment of their contributions to the spectra as it evolves. Figure 2c shows the two component spectra extracted from the spectra of 2b, and 2d shows their evolution with bias voltage. The good agreement between the extracted spectra and those of the pure materials indicates that MCR can accurately monitor spectral changes between the neutral and polaron states. We used MCR to monitor polaron formation directly in polymer/oxide heterojunctions, in order to detect structural and electronic changes within the polymer.

Figure 3a shows the effect of a series of bias pulses applied to Au/SiO$_2$(51)/P3HT(25)/Cr(2)/Au(10) junction on the Raman spectra of the junction, and 3b shows the results of the MCR analysis. The initial spectrum is characteristic of neutral P3HT as expected for the unbiased device. When the bottom Au electrode is biased at −5 V for a total of 56 seconds the P3HT polaron is formed and persists for tens of minutes or often hours with the device at open circuit. A positive pulse to the bottom Au electrode returns the polaron to its neutral form, and this process may be repeated many times. These results provide unequivocal evidence for redox processes within the molecular junction, despite its very thin dimensions (<100 nm), and absence of intentional solvent or ions. However, once the polaron is formed it becomes the more stable state, and the system relaxes rapidly to the polaron following a positive bias pulse (<10 s at open circuit), as shown in both the spectra and the relative contributions in Fig. 3. As shown in Fig. 4, the results are quite different if the structure is "inverted" to make a Au/P3HT(25)/SiO$_2$(51)/Cr/Au heterojunction, in which the only change is the order of the polymer and silica layers. In this case a negative bias has minimal effect, while a positive bias generates the polaron. Although polaron formation is rapid and repeatable for many cycles, the

Fig. 3 **a** Raman spectra obtained on a single Au/SiO$_2$(51)/P3HT(25)/Au(10) device during the series of bias pulses indicated, progressing from bottom to top. Times in seconds are the duration of voltage or OCP since the previous spectrum. Open circuit potential (OCP) indicates that the device was unhooked from the voltage source. Numbers to the left of spectra correspond to "spectrum #" in panel **b**. **b** Relative contributions of the two MCR components, from left to right. The MCR components were extracted from the spectra of panel **a**, and were very similar to those shown in Fig. 2c
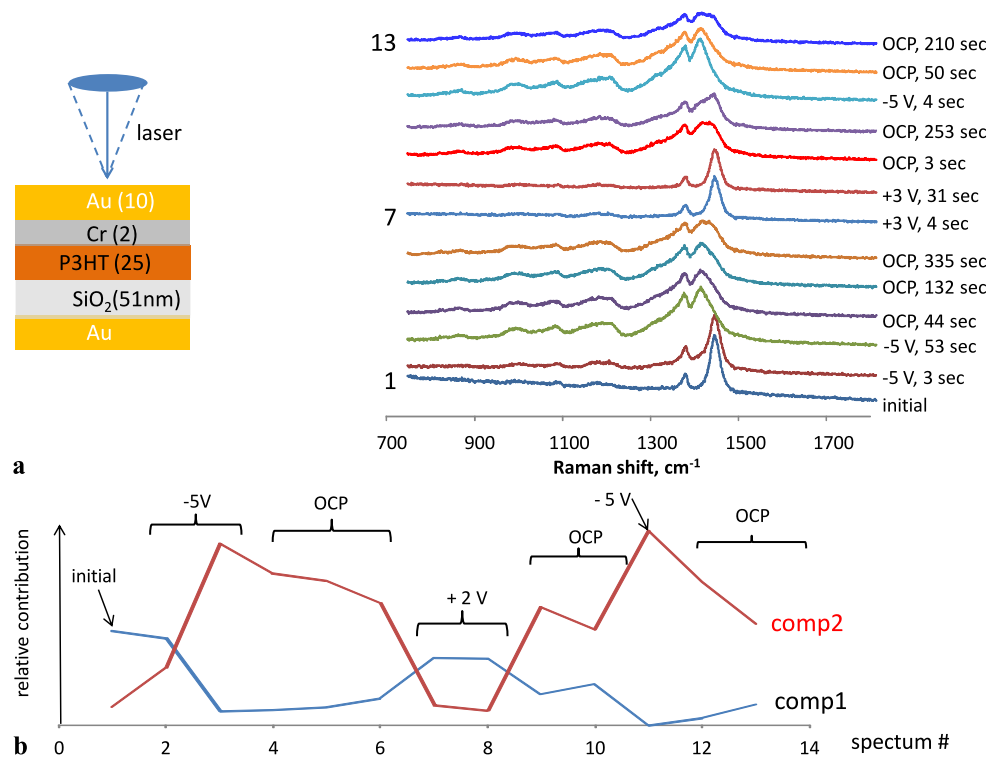
Fig. 4 **a** Raman spectra obtained on a single Au/P3HT(25)/SiO$_2$(51)/Cr(2)/Au(10) device during the series of bias pulses indicated, progressing from bottom to top. Times in seconds are the duration of voltage or OCP since the previous spectrum. Numbers to the left of spectra correspond to "spectrum #" in panel **b**. **b** Relative contributions of the two MCR components, from left to right. The MCR components were extracted from the spectra of panel **a**, and were very similar to those shown in Fig. 2c
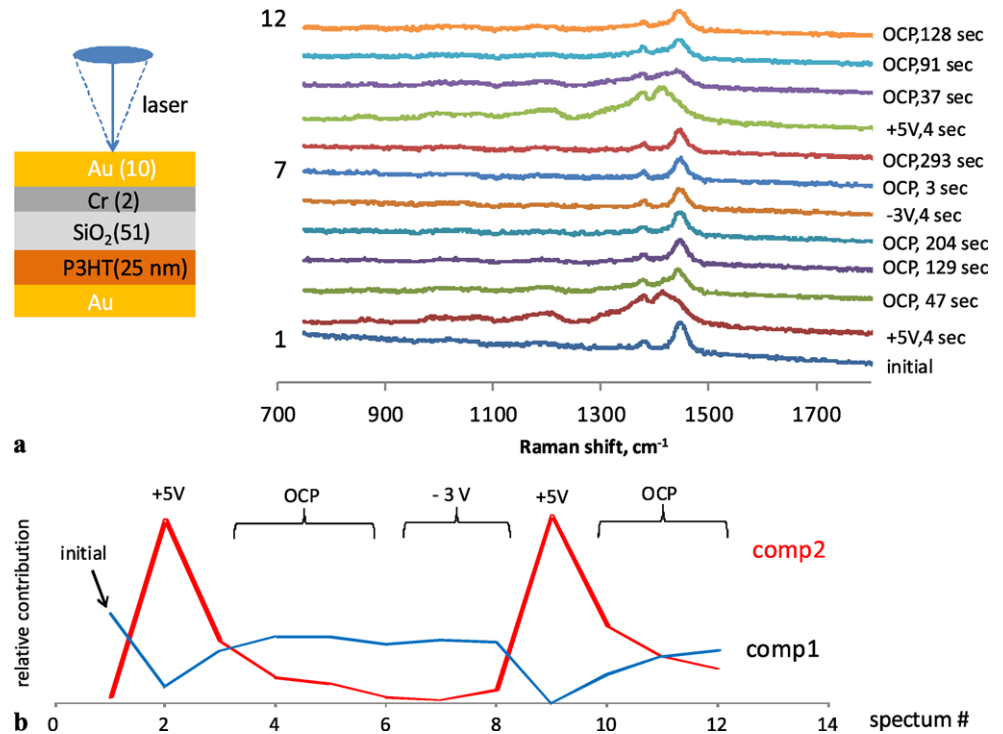
polaron is short-lived and decays back to the neutral state in a few seconds when the device is at open circuit. Even if the +5 V bias is held for 72 seconds to form the polaron, the spectrum rapidly reverts to that of the neutral polymer when the bias is removed. Since inversion of the P3HT and SiO$_2$ layers causes a dramatic change in polaron generation and stability, the interfaces between the layers and the contacts must be involved in the mechanism. An additional observation relevant to the switching mechanism is the complete cessation of polaron production if the devices
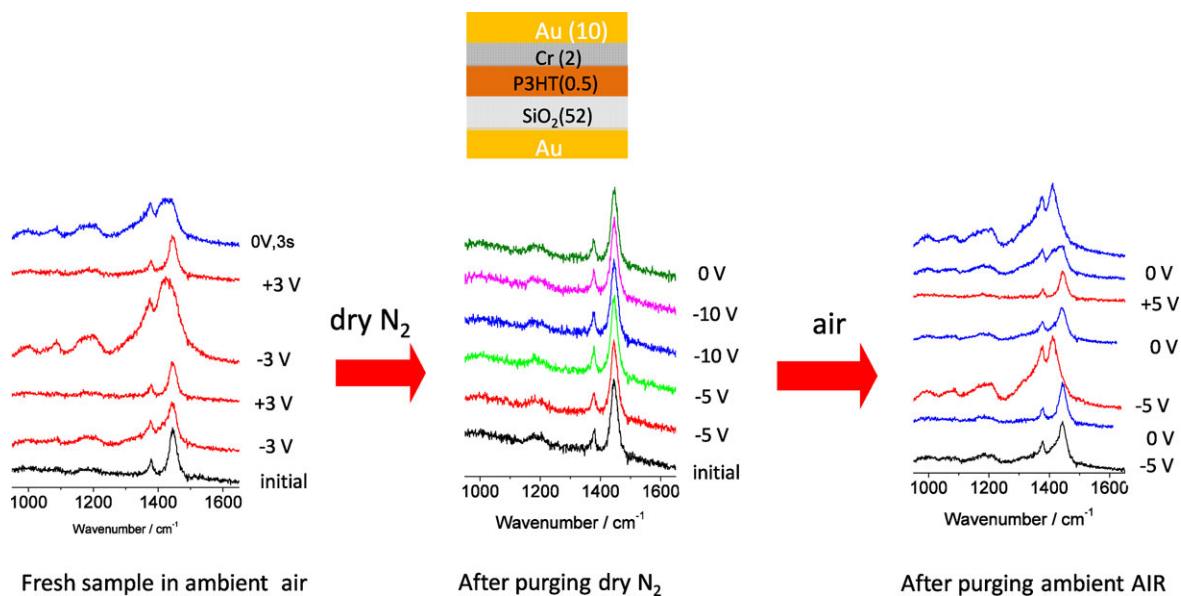
Fig. 5 Effect of humidity on polaron formation in a Au/SiO₂(52)/P3HT(25)/Cr(2)/Au(10) device. Each series progresses from bottom to top, with the bias values indicated. Sample was purged for several hours in dry N₂, and one hour in air

of Figs. 3 and 4 are placed in flowing, dry N₂ for 24 hours. As demonstrated in Fig. 5, a Au/SiO₂(52)/P3HT(25)/Cr/Au device similar to that of Fig. 3 forms stable polarons after −5 V bias in air, but shows no spectral change upon −5 or −10 V bias after prolonged exposure to dry N₂. When the device is exposed to air for ∼1 hour, reversible polaron formation at −5 V returns, and exposure to humidified N₂ also restores polaron formation for a −5 V bias. Exposure of a dried and inactive junction to N₂ saturated with acetonitrile did not restore polaron formation, implying that the conditions which promote ion motion are not sufficient to generate polarons. Clearly water is essential for polaron formation, for both the Au/SiO₂(50)/P3HT(25)/Cr/Au device and its "inverted" analog. It should be noted that the reversible polaron formation is not specific for the P3HT variant of polythiophene. The structurally similar regioregular poly(3,3‴-didodecyl-quaterthiophene), (PQT-12) [41–43] showed similar phenomena, which will be discussed separately.

The effect of electrode materials and oxide composition were investigated by substituting TiO₂, Al₂O₃, or Ta₂O₅ for the SiO₂ layer, and by replacing the bottom Au contact with a disordered form of carbon made from pyrolyzed photoresist [5, 44]. A carbon/SiO₂(50)/P3HT(25)/Cr(2)/Au(10) junction exhibited polaron formation when the carbon was biased at −3 or −5 V, but the polaron was short-lived, unlike the case for Au/SiO₂/P3HT/Cr/Au (Fig. 3). Furthermore, the polarons which are long-lived in the Au/SiO₂(50)/P3HT(25)/Cr(2)/Au(10) devices became short-lived if the only change was insertion of a second Cr layer

to make Au/Cr(2)/SiO₂(50)/P3HT(25)/Cr(2)/Au(10). The Raman spectra of a Au/Al₂O₃(50)/P3HT(25)/Cr/Au device showed no polaron formation, even for a −20 V bias on the bottom Au contact. Au/TiO₂(50)/P3HT(25)/Cr/Au and Au/Ta₂O₅(50)/P3HT(25)/Cr/Au devices exhibited polaron formation when the bottom Au was biased at −4 V, but the polarons were short-lived. In all the structures studied, exposure of the devices to dry N₂ prevents the polaron formation. The results of the entire collection of polymer/oxide devices are listed in Table 1, which compares the spectroscopic response of each device to various applied bias values.

Visual evidence for polaron formation and diffusion is provided in Fig. 6, which shows photographs of the top electrode of Au/SiO₂(50)/P3HT(25)/Cr/Au devices biased at 0 and −5 V. There is a difference in color of the top Au electrodes due to the underlying polaron, and the color changes propagate ∼25 µm away from the Au border. Spectra a and b were taken at the positions shown at zero bias, and show the expected neutral spectrum. The scale bars demonstrate the significant attenuation in Raman signal due to light absorption by the top electrode. With a −5 V bias, the spectrum of the P3HT under the Au electrode changes to that of the polaron, as expected (spectrum, 6c). Although spectrum 6d, taken near the top electrode border, does not obviously represent the polaron, the MCR analysis revealed a 1–5% contribution of polaron, indicating polaron diffusion away from the Au top electrode.

Table 1 Summary of device structures and behaviors

First layer	Second layer[a]	Bias[b]	Atmosphere	Polaron formed?	Polaron lifetime[c]	Designation
SiO$_2$	P3HT	−5 V	air	yes	long	Au/SiO$_2$(50)/P3HT(25)/Cr/Au
P3HT	SiO$_2$	+5 V	air	yes	short	Au/P3HT(25)/SiO$_2$(50)/Cr/Au
SiO$_2$	P3HT	−5 V	dry N$_2$	no		Au/SiO$_2$(50)/P3HT(25)/Cr/Au
P3HT	SiO$_2$	+5 V	dry N$_2$	no		Au/P3HT(25)/SiO$_2$(50)/Cr/Au
SiO$_2$	P3HT	+5 V	CH$_3$CN	no		Au/SiO$_2$(50)/P3HT(25)/Cr/Au
SiO$_2$	P3HT	−5 V	air	yes	short	carbon/SiO$_2$(50)/P3HT(25)/Cr/Au
SiO$_2$	P3HT	−5 V	dry N$_2$	no		carbon/SiO$_2$(50)/P3HT(25)/Cr/Au
Al$_2$O$_3$	P3HT	−20 V	air	no		Au/Al$_2$O$_3$(50)/P3HT(25)/Cr/Au
TiO$_2$	P3HT	−5 V	air	yes	short	Au/TiO$_2$(50)/P3HT(25)/Cr/Au
Ta$_2$O$_5$	P3HT	−5 V	air	yes	short	Au/Ta$_2$O$_5$(50)/P3HT(25)/Cr/Au

[a]Junction was completed with a top contact of 2 nm of Cr and 10 nm of Au

[b]Bottom electrode relative to top contact

[c]Polaron formation under the indicated bias and lifetime at open circuit were determined with Raman spectroscopy

Fig. 6 *Center*: differential interference contrast (i.e. Nomarski) images of the top of a Au/SiO$_2$(50)/P3HT(25)/Cr(2)/Au(10) device before and after a −5 V bias was applied. Spectra **a** and **b** were obtained at the indicated locations, with the scale bars indicating the difference in Raman intensity. The lower image was obtained after several minutes with a −5 V bias applied to the bottom electrode, spectra **c** and **d** obtained at the indicated locations
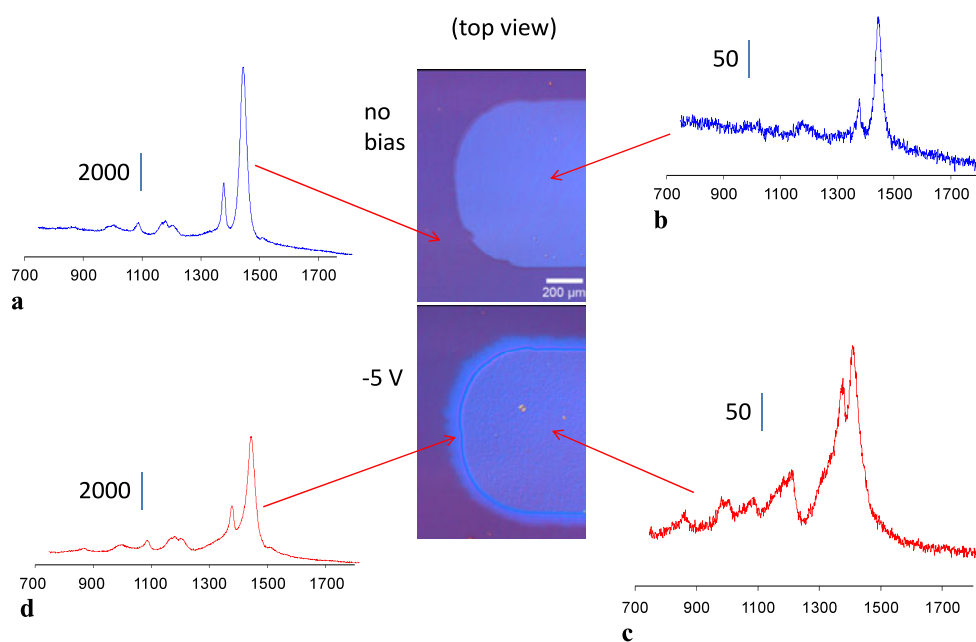
4 Discussion

The present results and past reports [3, 4, 6, 30] clearly show that it is possible for a voltage bias on a molecular junction to induce redox reactions in a molecular layer, TiO$_2$, or a conducting polymer film such as polythiophene. Such reactions are possible even in devices with active thicknesses in the 10–75 nm range, and can be monitored by UV-vis absorption and Raman spectroscopy. Table 1 indicates that the degree of oxidation of P3HT and the stability of the oxidized form are strongly dependent on the composition of the junction, notably the electrode materials, the oxide, and the presence of water. Familiar analogs of the molecular heterojunc-

tion are shown in Fig. 7, and these structures are relevant to the discussion. The device structure shown in Fig. 7a is the parallel plate capacitor, in which an applied bias generates charge separation across an insulating dielectric (I). When two dielectric layers are present, the capacitance is a function of the two dielectric constants and their thicknesses, as if there were two capacitors in series. Figure 7b shows the case of a conducting polymer replacing one dielectric layer, with the polymer initially in its neutral, nonconducting state. A positive bias adjacent to the polymer can result in charge transfer into the polymer, in this case causing partial oxidation of the polymer. This process is often called "electrosta-
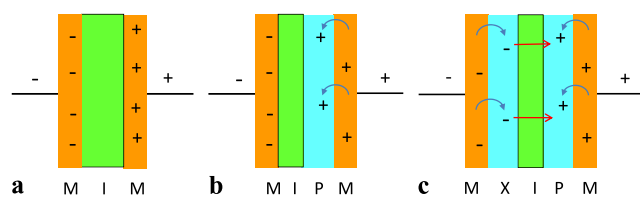
Fig. 7 Schematics of metal-insulator-polymer thin layer devices. **a** Parallel plate capacitor with bias applied; **b** metal-insulator-polythiophene-metal device in which the bias has oxidized the polymer and an image charge stabilizes the resulting polaron; **c** complete electrochemical cell with an added redox agent (X) which can accept electrons. If X is H_2O, reduction generates OH^-, which can migrate to stabilize the polaron

tic doping" because an organic layer can be oxidized to its conducting state, and the process is the basis of most organic field effect transistors [8, 45, 46]. For example if layer 2 is polythiophene, it may be oxidized to its conducting polaron, with the charges on these polarons balanced by the image charge on the opposing electrode, as shown in Fig. 7b. In the absence of mobile ions, the charge induced in the polythiophene layer is sustained only under applied bias, and "discharges" rapidly when the applied bias is removed. Figure 7c adds to 7b a second redox system with mobile ions, and contains all the elements of a conventional electrochemical cell, such as a common battery. An applied bias of sufficient magnitude causes reduction at one electrode and oxidation at the other, and ions move in response to the resulting electric field. These ions compensate the charge at each electrode and remove the electric field profile within the device. The absence of an internal electric field in a "charged" cell results in a device which is stable at open circuit. The OFET literature refers to this process as "electrochemical doping", and it can be distinguished from "electrostatic doping" both by its strong dependence on mobile ions and by the effect of electrode geometry [9, 46]. Notice that the opposite polarities required for polaron formation evident from Figs. 3 and 4 are consistent with the requirement that the electrode adjacent to the polythiophene is positively biased, as shown for the right electrode in Figs. 7b and 7c.

For all of the P3HT/oxide devices listed in Table 1, removing water prevented polaron formation, and therefore inhibited the desired resistance switching phenomenon. Water can support ion motion, but it can also act as a redox agent; in this case the reduction of water to H_2 and OH^- could be the counter-reaction for oxidation of P3HT. Note also that the reversal of the electrodes between entry 1 and entry 2 of Table 1 caused a major change in the stability of the polaron. When an Au/SiO_2 interface was present, the polaron was long lived, while the insertion of Cr between Au and SiO_2 resulted in short-lived polarons. Furthermore, addition of acetonitrile vapor to a previously dried device did not restore polaron formation, even though acetonitrile is commonly used as a solvent for electrolytes and should support

ion motion. These observations permit proposal of an electrochemical doping mechanism based on water reduction. The reduction of water at the surface of a metal electrode is considered "electrocatalytic", meaning that chemisorption of water is required for efficient reduction and H_2 generation. When SiO_2 is in direct contact with Au that is biased negatively, reaction (2) can occur:

$$H_2O + e(Au) \rightarrow \frac{1}{2}H_2 + OH^- \tag{2}$$

The hydrogen is present either as molecular H_2 or as chemisorbed H atoms on the Au surface. The OH^- ion is likely to migrate in the electric field, and then to compensate for the charge of the P3HT polaron, making a complete cell reaction:

$$H_2O + P3HT \rightarrow \frac{1}{2}H_2 + P3HT^+ + OH^- \tag{3}$$
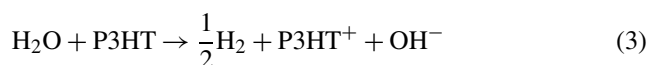
Chromium is much less electrocatalytically active for H_2O reduction than Au, due to formation of Cr oxide, which only weakly adsorbs water or hydrogen. Similarly, disordered carbon does not exhibit electrocatalytic activity for H_2O reduction in comparison with Au. In these cases the polaron is formed but is short-lived, presumably due to the fact that no OH^- is formed to compensate the cationic P3HT polaron. Note that the substitution of carbon or Cr for Au in devices otherwise identical to $Au/SiO_2(50)/P3HT(25)/Cr(2)/Au(10)$ resulted in a dramatic decrease in polaron lifetime, due to the absence of electrocatalytic H_2O reduction. The reasons for the absence of polaron formation in the case of Al_2O_3 and the short polaron lifetime for TiO_2, and Ta_2O_5 as the oxides are not clear, since there is an Au/oxide interface in all cases (entries 8–10 in Table 1). A possible reason is the affinity difference of these oxides for water. SiO_2 is significantly more hygroscopic than the other oxides, and the low water activity without SiO_2 may be responsible for the short-lived polaron. Overall, the $P3HT/SiO_2$ heterojunctions are examples of "electrochemical doping" in which water reduction plays a vital role as the redox counter reaction. Thus polaron stability is a result of the formation of chemisorbed hydrogen on Au or OH^- migration. These results clearly indicate the importance of interfaces to the resistive switching observed in conducting polymer/TiO_2 devices, as well as the presence of redox active components in addition to the polymer itself.

The case of carbon/fluorene/TiO_2/Au devices reported previously [3, 4, 6] and described briefly in the introduction is quite distinct from the polymer devices, since fluorene is unlikely to undergo redox reactions. The change in conductance with a bias applied to the Au/TiO_2 interface was associated with reduction of TiO_2, as has been reported for water-catalyzed photoreduction of TiO_2 [47, 48]. The resistance switching in fluorene/TiO_2 devices was completely suppressed in a dry atmosphere [1], while switching

in polypyrrole/TiO_2 junctions was unchanged or stronger with water absent [7]. Based on the current polymer results, the relatively short retention of fluorene/TiO_2 devices may be analogous to the case of Fig. 7b, in which the absence of a second redox couple results in a large internal electric field and short retention. It is difficult to oxidize either water or carbon at the carbon/fluorene interface, so a companion reaction to TiO_2 reduction is not available. As a consequence, the conductive TiO_{2-x} phase can form, but it is metastable, returning to its insulating TiO_2 form in a few tens of minutes. The role of defects and conducting filaments has been considered in some detail for resistance switching in metal oxides, particularly "memristor" structures based on TiO_2. Oxygen vacancy migration has been proposed to generate conducting channels of TiO_{2-x} "suboxides", and these channels may be responsible for the observed conductance changes [22–26, 49]. Note that the H_2O-dependent conductance change associated with reaction (1) may represent a different mechanism for forming TiO_{2-x} from that proposed for memristors, but both routes involve reduction of Ti^{IV} centers to Ti^{III} or Ti^{II}.

In the case of conducting polymers such as polythiophene and polypyrrole, such channels might take the form of a "track" of polarons with conductivities much higher than the surrounding neutral polymer. Spectroscopy uses a "macroscopic" sampling area relative to the size of a polaron, and hence provides a spatially averaged indication of polaron formation. Although spectroscopy definitively establishes macroscopic polaron formation under applied bias, it does not provide a direct probe of the presence or absence of conducting channels. Our current research into resistance switching in conducting polymer memory devices correlates conductance changes with spectroscopic monitoring of the polymer oxidation state, with materials and electrodes chosen not only to facilitate polymer redox processes but to maximize changes in device resistance.

References

1. J.C. Scott, L.D. Bozano, Adv. Mater. **19**, 1452 (2007)
2. R. Waser, R. Dittmann, G. Staikov, K. Szot, Adv. Mater. **21**, 2632 (2009)
3. J. Wu, R.L. McCreery, J. Electrochem. Soc. **156**, P29 (2009)
4. J. Wu, K. Mobley, R. McCreery, J. Chem. Phys. **126**, 24704 (2007)
5. R. McCreery, J. Wu, R.J. Kalakodimi, Phys. Chem. Chem. Phys. **8**, 2572 (2006)
6. A. Nowak, R. McCreery, J. Am. Chem. Soc. **126**, 16621 (2004)
7. S. Barman, F. Deng, R. McCreery, J. Am. Chem. Soc. **130**, 11073 (2008)
8. M.J. Panzer, C.D. Frisbie, Adv. Funct. Mater. **16**, 1051 (2006)
9. L.G. Kaake, Y. Zou, M.J. Panzer, C.D. Frisbie, X.Y. Zhu, J. Am. Chem. Soc. **129**, 7824 (2007)
10. J.H. Zhao, D.J. Thomson, M. Pilapil, R.G. Pillai, G.M.A. Rahman, M.S. Freund, Nanotechnology **21**, 134003 (2010)
11. G.M.A. Rahman, J.-H. Zhao, D.J. Thomson, M.S. Freund, J. Am. Chem. Soc. **131**, 15600 (2009)
12. J.H. Zhao, D.J. Thomson, R.G. Pillai, M.S. Freund, Appl. Phys. Lett. **94**, 092113 (2009)
13. R.G. Pillai, J.H. Zhao, M.S. Freund, D.J. Thomson, Adv. Mater. **20**, 49 (2008)
14. J.H. Krieger, S.V. Trubin, S.B. Vaschenko, N.F. Yudanov, Synth. Met. **122**, 199 (2001)
15. S.G. Robinson, D.H. Johnston, C.D. Weber, M.C. Lonergan, Chem. Mater. **22**, 241 (2010)
16. H.J. Lee, Z.X. Jin, A.N. Aleshin, J.Y. Lee, M.J. Goh, K. Akagi, Y.S. Kim, D.W. Kim, Y.W. Park, J. Am. Chem. Soc. **126**, 16722 (2004)
17. J.L. Bredas, R. Silbey, D.S. Boudreaux, R.R. Chance, J. Am. Chem. Soc. **105**, 6555 (1983)
18. J. Nowotny, T. Bak, M.K. Nowotny, L.R. Sheppard, J. Phys. Chem. C **112**, 602 (2008)
19. J. Nowotny, T. Bak, M.K. Nowotny, L.R. Sheppard, J. Phys. Chem. C **112**, 590 (2008)
20. P. Knauth, H.L. Tuller, J. Appl. Phys. **85**, 897 (1999)
21. D. Mardare, C. Baban, R. Gavrila, M. Modreanu, G.I. Rusu, Surf. Sci. **507–510**, 468 (2002)
22. S. John Paul, D.P. Matthew, J.J. Yang, A. Shaul, A.L.D. Kilcoyne, M.-R. Gilberto, R.S. Williams, Adv. Mater. **22**, 3573 (2010)
23. D.B. Strukov, R.S. Williams, Appl. Phys. A, Mater. Sci. Process. **94**, 515 (2009)
24. N. Gergel-Hackett, B. Hamadani, B. Dunlap, J. Suehle, C. Richter, C. Hacker, D. Gundlach, IEEE Electron Device Lett. **30**, 706 (2009)
25. J.J. Yang, M.D. Pickett, X. Li, D. Ohlberg, D. Stewart, R.S. Williams, Nat. Nanotechnol. **3**, 429 (2008)
26. D.B. Strukov, G.S. Snider, D.R. Stewart, R.S. Williams, Nature **453**, 80 (2008)
27. R. McCreery, Method for conductance switching in molecular electronic junctions, U.S. Patent # 6,855,950 (2005)
28. A.O. Solak, S. Ranganathan, T. Itoh, R.L. McCreery, Electrochem. Solid-State Lett. **5**, E43 (2002)
29. A.O. Solak, L.R. Eichorst, W.J. Clark, R.L. McCreery, Anal. Chem. **75**, 296 (2003)
30. A.P. Bonifas, R.L. McCreery, Chem. Mater. **20**, 3849 (2008)
31. F. Anariba, S.H. DuVall, R.L. McCreery, Anal. Chem. **75**, 3837 (2003)
32. Y. Gao, T.P. Martin, E.T. Niles, A.J. Wise, A.K. Thomas, J.K. Grey, J. Phys. Chem. C **114**, 15121 (2010)
33. E. Klimov, W. Li, X. Yang, G.G. Hoffmann, J. Loos, Macromolecules **39**, 4493 (2006)
34. G. Louarn, M. Trznadel, J.P. Buisson, J. Laska, A. Pron, M. Lapkowski, S. Lefrant, J. Phys. Chem. **100**, 12532 (1996)
35. M. Baibarac, M. Lapkowski, A. Pron, S. Lefrant, I. Baltog, J. Raman Spectrosc. **29**, 825 (1998)
36. A.S. Dhoot, G.M. Wang, D. Moses, A.J. Heeger, Phys. Rev. Lett. **96**, 246403 (2006)
37. D. Ofer, R.M. Crooks, M.S. Wrighton, J. Am. Chem. Soc. **112**, 7869 (1990)
38. N. Vukmirovic, L.-W. Wang, J. Phys. Chem. B **113**, 409 (2008)
39. E.L. Ratcliff, J.L. Jenkins, K. Nebesny, N.R. Armstrong, Chem. Mater. **20**, 5796 (2008)
40. J. Hou, Z. Tan, Y. Yan, Y. He, C. Yang, Y. Li, J. Am. Chem. Soc. **128**, 4911 (2006)

41. B.S. Ong, Y. Wu, P. Liu, S. Gardner, Adv. Mater. **17**, 1141 (2005)
42. Y. Wu, P. Liu, S. Gardner, B.S. Ong, Chem. Mater. **17**, 221 (2004)
43. B.S. Ong, Y. Wu, P. Liu, S. Gardner, J. Am. Chem. Soc. **126**, 3378 (2004)
44. S. Ranganathan, R.L. McCreery, S.M. Majji, M. Madou, J. Electrochem. Soc. **147**, 277 (2000)
45. X. Yu, C. Jeong Ho, L. Jiyoul, P.P. Ruden, C.D. Frisbie, Adv. Mater. **21**, 2174 (2009)
46. M.J. Panzer, C.D. Frisbie, J. Am. Chem. Soc. **129**, 6599 (2007)
47. S.H. Szczepankiewicz, J.A. Moss, M.R. Hoffmann, J. Phys. Chem. B **106**, 7654 (2002)
48. S.H. Szczepankiewicz, J.A. Moss, M.R. Hoffmann, J. Phys. Chem. B **106**, 2922 (2002)
49. T. Driscoll, J. Quinn, S. Klein, H.T. Kim, B.J. Kim, V.P. Yu, M.D. Ventra, D.N. Basov, Appl. Phys. Lett. **97**, 093502 (2010)